DAYLIGHT PHOTOLUMINESCENCE OF SILICON SOLAR PANELS IN OPERATION BY ELECTRICAL MODULATION

C. Terrados[1,2], D. González-Francés[1], K.P. Sulca[1], C. de Castro[1], M.A. González[1], O. Martínez[1]*
(1) GdS-Optronlab group, Dpto. Física de la Materia Condensada, Universidad de Valladolid, Edificio LUCIA, Paseo de Belén 19, 47016 Valladolid (Spain)
(2) Solar and Wind Feasibility Technologies (SWIFT). Escuela Politécnica Superior, Universidad de Burgos. Avda. Cantabria s/n 09006 Burgos (Spain)
*oscar.martinez@uva.es

ABSTRACT: Daylight Photoluminescence (dPL) has appeared in recent years as a useful tool for the inspection of solar panels, allowing for the identification of several kind of defects with good spatial resolution. The commutation between two states (On and Off) is usually necessary for the filtration of the ambient light. Several practical solutions have been implemented to do this kind of commutation, both electrically or optically. Here we explore in detail the method consisting on the electrical commutation using an electronic device connected in parallel to an adequate number of panels of a string, allowing to inspect the panels during operation, which is contactless once the electrical device is installed. The method can be also applied for the inspection of whole strings, in this case the electronic device is connected in series to the string to be inspected. The advantage of the method is the very fast commutation of the state of the string, between the MPP state and a state at/or very close to OC conditions. The values of the On and Off signals, the process and quality of the images, and the response of the inverter have been checked.
Keywords: Photoluminescence, daylight, inspection, PV panels

1 INTRODUCTION

Among the inspection techniques for defect characterization of Si solar panels, luminescence techniques provide a good spatial resolution and allows for the identification of several types of defects [1-3]. Electroluminescence (EL) inspection with Si cameras in complete dark ambient has been traditionally performed as a standard testing technique and is very well suited as an approval testing technique prior the Si solar panels are installed on a PV plant. Also dark EL (nEL) are used extensively for the inspection of the solar panels installed on a solar PV plant, but the strict dark conditions required when using Si cameras is a high disadvantage, since requires working during the night, or dismount the panels to be inspected on a laboratory or in a dark ambient in a mobile van [3-5]. Daylight luminescence techniques has been developed in recent years, with the possibility to inspect the panels on-site, and the aim to arrive to a massive inspection of the PV plants. Daylight EL (dEL) has been developed in recent years [6-10], requiring cameras with a high QE in the near IR range, as well as methods for filtering the ambient light. The dEL image is usually obtained by subtracting the signal when the panel is powered ("On" state) from when the panel is not powered (open circuit conditions –OC, "Off" state). On the other hand, daylight Photoluminescence (dPL) have the advantage of not needing a power source, since uses the sun as the light excitation source. However, it usually still requires two states ("On" and "Off" conditions) to distinguish the light coming from the panels form the ambient light, which still require electrical or optical contacts to be performed [11, 12]. The capability to made dPL in the more contactless way possible will be very beneficial for the inspection of a large amount of Si panels on-site on the PV plants.

We have previously developed a dPL system that allows to commutate the panels between the open circuit – OC ("On" state) and short circuit – SC ("Off" state) points of the I-V curve of the panel [10]. In OC conditions, the photogenerated carriers can recombine radiatively, producing a luminescence signal. In SC conditions, most of the photogenerated carriers scape through the electrical circuit and the luminescence signal is reduced. The difference between the two states allows to extract the PL signal [10, 13]. In our system we used an InGaAs camera, specific filters to filtrate as much ambient light as possible, and an electronic device that rapidly commutes between OC and SC conditions and is also synchronized with the InGaAs camera to collect the signal in both states ($dPL_{OC/SC}$). For the practical realization of the $dPL_{OC/SC}$ measurements, the whole string was disconnected from the PV plant, and the individual Si panels from the string. The electronic device was then connected to each of the individual panels, in a contact way. The electronic device itself serves as the electric connection for the SC condition [10].

Different approaches have been also used to commutate the panels between two states, to have a large difference in the PL emission. For this purpose, electrical or optical commutations have been developed [11,12]. In the case of optical commutation, a LED can be placed to cover a solar cell, to inspect one panel, or several optical modulators (LEDs) to inspect a whole string [13, 14]. In this case, although the system can be denoted as contactless, and the optical commutation can be very quickly, the optical modulators should be putted on some of the solar cells, and then removed, which still results in an operation procedure not really simple. Also, not the complete panel or string can be inspected. Different approaches in the case of electrical commutation have been also developed in the last years, mainly through the use of the inverter to produce the change between two states. Some developments use the sweep of the I-V performed by some inverters [15]. Others, force the inverter to change between two states, which is not a quickly way [16]. More recently, a new development was performed by modifying the inverter itself to produce the change between the two states in a quickly way [11]. However, in these cases, the dPL image is obtained by forcing the inverter to operate at two voltage points or it is necessary to modify the inverter to introduce this capability.

Here, we show a modification of our $dPL_{OC/SC}$ method

by electrical commutation [10] using an electronic device to force the panels itself to work at two different points of the I-V curve, one at the maximum power point (MPP) at which the string usually works due to the maximum power point track (MPPT) function of the inverters, and thus with high Intensity (I_{MPP}) ("Off" state), and another at high voltage and thus low intensity (near or at the OC condition) ("On" state). The method can also be applied to a whole string of S panels; in this case, one string (of p strings connected in parallel to an inverter) is forced by means of the electronic device to work at these two points of the I-V curve.

In this communication we show the results corresponding to the disconnection of N panels from a string of 20 panels, and the response of two different inverters. A demonstration test was also carried out for the case of inspecting a whole string, using a micro-inverter working with two parallel strings of only one panel each.

2 METHODOLOGY

2.1 Electrical commutation

Let´s consider a string of S panels connected in series with the inverter. The electrical commutation proposed here is performed by using and electronic device which is inserted in parallel with an adequate number of panels (N), which force N panels to be disconnected from the rest of the string, such that the inverter is now working with only S–N panels. This is performed very quickly, and controlled by remote control using a computer and wireless connection. Due to the very quick change, the inverter is supposed to not be aware of the change, this means that the rest of the string (S–N panels) works at a higher voltage, and thus the operation point of the rest of the string moves to a much higher voltage in the I-V curve, very close to V_{OC} if the number of panels is properly selected, thus with a much lower current than before. This procedure is thus used to commutate the state of the panels between two points with a large difference in intensity, Fig. 1, avoiding forcing the inverter itself. By using the electronic device it is possible to make a very fast commutation, electrically connecting and disconnecting the N panels from the rest of the string, allowing for the obtention of a dPL image by subtracting the On and Off signals, which are obtained at nearly the same external irradiation conditions, thus favoring the quality of the obtained dPL image, and repeating the process as many times as desired to filtrate as much as needed the ambient light.

The method can be extended to inspect an entire string in operation. In this case, for a configuration with p strings connected in parallel to the MPPT of the inverter, it is possible to connect the electronic device in series with the string(s) to be inspected. Here, the Off state will be again the one at the MPP where the p strings normally operate, and therefore with a high current (I_{MPP}) drawn from all the strings, and which is obtained in this case when the electronic device is activated. In order to obtain an On state, the electronic device is deactivated, thus disconnecting the inspected string from the rest of the p strings, thereby forcing this string to work at OC conditions. Remotely disconnecting the string does not change the voltage in the MPPT of the inverter, while the change in the current drawn from the remaining p-1 strings connected to the MPPT of the inverter would be small, depending on the number (p) of strings connected in parallel to the inverter.

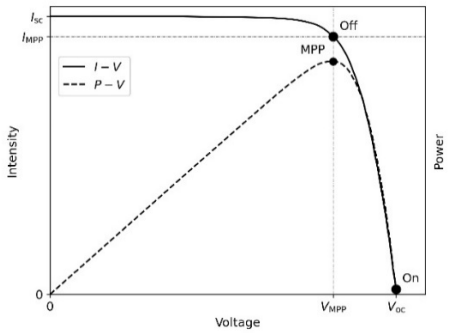

Figure 1: I-V curve showing the two points for the electrical commutation. The Off state is the normal operation point of the string (MPP point) due to the MPPT function of the inverter.

2.2 Materials and methods

We used an InGaAs camera, Hamamatsu C12741-03, with 640 x 512 pixels and 14 bits´ resolution. Exposure times range from 1 µs to 1 s, which enables acquisition to be adapted to the different lighting conditions. A Kowa short-wave infrared (SWIR) optical system with 16 mm focal length was used for image acquisition. A SWIR bandpass filter – centred around 1160 nm with a bandwidth of 150 nm and a transmittance close to 90% – is used.

The electronic device used to switch the polarization states consists of a 1700 V IGBT (IXGN100N170 model), which is sufficient for a complete string operating at 1500 V and carrying 10 A.

Probes were performed using a whole string of 20 modules (mc-Si, ND-AR 330 W model from Sharp), with V_{OC} = 45.5 V, I_{SC} = 9.4 A, V_{MPP} = 37.1 V, I_{MPP} = 8.9 A (at STC). We tested two different inverters. Inverter 1 is a SUN 3Play TL–20 kW Ingeteam inverter, with an operating range of 560–820 V. Inverter 2 is a Fronius Symo 4.5-3-M model with a working range of 150–1000 V. We also used a micro-inverter (APS DS3 880W 230V model) capable of working with two panels in parallel, in order to demonstrate the method for inspecting whole strings in operation. Effective voltage and current signals at the exit of the inverter were recorded using Fluke 80K-40 and Fluke 80i-110s probes, respectively. Voltage and current measurements are shown as 5-second time segments.

2.2 Subtraction procedure

The subtraction procedure involves subtracting the On signal vis-à-vis the Off signal for each pixel, and accumulating the signal differences over a certain number of cycles (nc). Due to the presence of ambient light (background), the intensity signal (for both On and Off periods) can be very large and may even saturate the sensor, while the On–Off signal difference can be very small. To avoid saturating the sensor, it is usual to play with the aperture of the camera objective. Exposure time (t_{exp}) can also be varied. For fast switching, t_{exp} is usually chosen in the range [3-12] ms, and the aperture is modified accordingly. For the InGaAs camera used – with a resolution of 14 bits – the signal is limited to 16,384 grey levels (counts).

Our software is programed to store all the images, both for the On and Off periods, for the nc cycles. 2 x nc images

are thus obtained. The software is also programed to make the difference $Signal_{(1)}^{k} = On_{(1)}^{k} - Off_{(1)}^{k}$ for each pixel k, store it as $Signal_{(accum,1)}^{k}$, and then make the difference $Signal_{(2)}^{k} = On_{(2)}^{k} - Off_{(2)}^{k}$ and add it to the previous accumulated value. A final image is obtained with the final $Signal_{(accum,nc)}^{k}$ over the nc cycles for all the pixels, giving the resulting dEL/dPL image.

In order to quantify the quality of the images obtained, the signal-to-noise ratio SNR_{avg} was calculated from the 2 x nc partial images, according to the expression given in [17].

3 RESULTS

3.1 Inspection of S–N panels of a string

For the probed string of 20 panels, according to their V_{OC} and V_{MPP} values, and to the working range of Inverter 1, the maximum number of panels that can be electrically disconnected but maintain the inverted working should be such that Voc x (20–N) ≥ 560, thus is N=7. This would be the case for an irradiance of 1000 W/m^2 and 20ºC (STC). dPL measurements on this string by disconnecting N panels from the string, with N from 1 to 6, have been performed (denoted as $dPL_{20/N}$). Figure 2(a) shows the dPL image of one defective panel obtained with the use of the electronic device in parallel with N=6 panels ($dPL_{20/6}$), for G = 1020 W/m^2 (the inverter is thus working with 14 panels in the Off periods). An exposure time of 5 ms and 300 On/Off cycles has been used. The On and Off signals can largely fluctuate (irradiation fluctuations due to clouds, for instance) and the On–Off signal differences are usually small (less than 15 counts in these measurements, Fig. 2(b), which makes the image obtention process not easy), but still enough to obtain a good quality dPL image, with a relatively large SNR_{avg} value of 17.3 [17]. The dPL image obtained by inspecting this isolated panel commuting between OC (On) and SC (Off) conditions ($dPL_{OC/SC}$) for the same irradiation conditions and camera parameters gives a SNR_{avg} value of 23.8, Fig.3(a), and nearly exactly the same visual information as the $dPL_{20/6}$ case. On the other hand, the dEL image obtained for the same irradiation conditions (G = 1020 W/m^2) and camera parameters (t_{exp}=5 ms, nc=300), injecting a current of 9 A, give a larger SNR_{avg} value of 43.2, Fig.3(b). The same defective cells are detected, although the level of information is different. The difference between the dEL and the dPL information has been discussed in some papers [12, 18, 19]. In any case, it can be observed that the defective cells are distinguished in both cases.

Fig.2(c) shows the voltage and current measured at the output of the inverter during the first cycles of the $dPL_{20/6}$ measurement, showing the commutation between the On and Off states. A good square wave modulation is obtained for the current intensity, between 0 and ~8 A, while the voltage (that of the inverter) – which is modulated according to the electrical grid value– shows no important changes. The maximum values of the current intensity (Off periods) (~ 8 A) corresponds well to the high irradiation conditions of the measurement (I_{MPP} = 8.9 A at STC). It is also interesting to note that the current intensity modulation was observed to be constant all along the $dPL_{20/6}$ measurement, that indicating that both On and Off states are well fixed during the measurement. In fact, it can be clearly seen that the mean On–Off signal differences are fully constant, Fig. 2(b). The good quality of the obtained $dPL_{20/6}$ image is thus attributed to the large difference in current intensity values between the On and Off periods (ΔI ~ 8 A), the fast switching between the two periods, and the perfect square modulation.

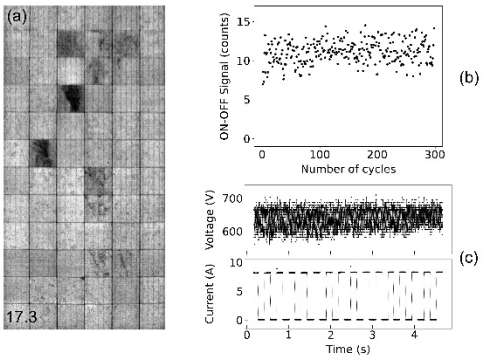

Figure 2: (a) dPL image of an individual panel of the string of S=20 panels connected with Inverter 1, with the electronic device connected in parallel with N=6 panels ($dPL_{20/6}$) (G = 1020 W/m^2, t_{exp}=5 ms, nc=300) (the calculated SNR_{avg} value is indicated on the bottom-left corner); (b) On–Off signal differences as a function of the number of cycles; (c) voltage and current values measured at the output of the inverter during the first cycles of the measurement

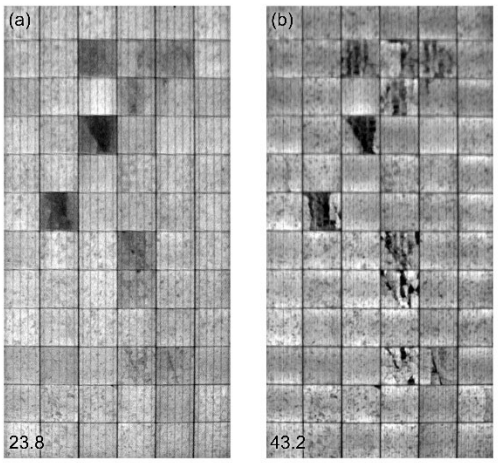

Figure 3: (a) $dPL_{OC/SC}$ and (b) dEL images of the same individual panel as shown in Fig. 2(a) (G = 1020 W/m^2, t_{exp}=5 ms, nc=300; $I_{current}$ = 9 A for the case of the dEL image)

Figure 4(a) shows the dPL image obtained for the same panel of this string of 20 modules, with the use of the electronic device in parallel with N=3 panels ($dPL_{20/3}$), for G = 1020 W/m^2. Again, an exposure time of 5 ms and 300 On/Off cycles has been used. The quality of the image has largely degraded, with an SNR_{avg} value decreasing to 13.2. The On–Off signal differences, as well as the voltage and current measured at the output of the inverter during the first cycles of this $dPL_{20/3}$ measurement, are shown in Fig. 4 (b) and (c), respectively. The current intensity modulation was observed not to be constant all along the $dPL_{20/3}$ measurement, with an Off state not fixed. This is reflected in the On–Off signal differences, which decreases monolithically to zero, Fig. 4(b). Thus, the bad quality of the obtained $dPL_{20/3}$ image is due to the small difference in current intensity values between the On and Off periods, with a large imperfect square modulation.

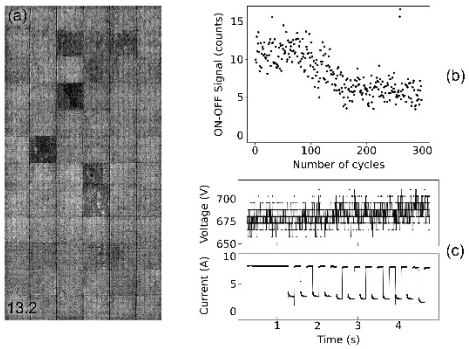

Figure 4: (a) dPL image of the same individual panel of the string of S=20 panels connected to Inverter 1, with the electronic device connected in parallel with N=3 panels ($dPL_{20/3}$) (G = 1020 W/m^2, t_{exp}=5 ms, nc=300); (b) On–Off signal differences as a function of the number of cycles; (c) voltage and current values measured at the output of the inverter during the first cycles of the measurement

3.2 Response of the inverter

The $dPL_{S/N}$ procedure has been checked for two different inverters, in order to study the inverter response and their effect on the obtained images. Fig. 5(a) shows the $dPL_{20/6}$ image obtained by using in this case Inverter 2, for the same conditions (G = 1020 W/m^2, t_{exp} = 5 ms, nc = 300). The On–Off signal differences, as well as the voltage and current measured at the output of the inverter during the first cycles of this $dPL_{20/3}$ measurement, are shown in Fig. 5 (b) and (c), respectively. It can be seen now a quite different response of the inverter, which should be ascribed to the presence of capacitors, and the corresponding discharge processes. In spite of this, the $dPL_{20/6}$ image obtained are still good enough (SNR_{avg} = 16.6) to clearly observe almost the same defective cells as with Inverter 1.

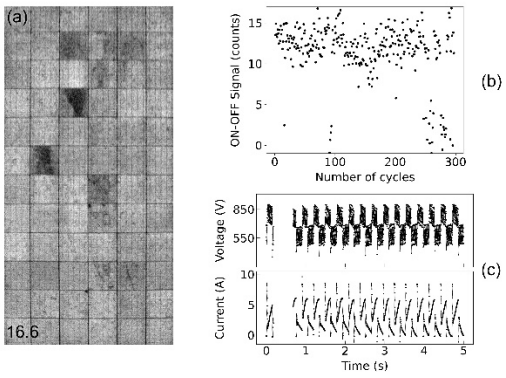

Figure 5: (a) dPL image of the same individual panel of the string of S=20 panels connected with Inverter 2, with the electronic device connected in parallel with N=6 panels ($dPL_{20/6}$) (G = 1020 W/m^2, t_{exp}=5 ms, nc=300); (b) On–Off signal differences as a function of the number of cycles; (c) voltage and current values measured at the output of the inverter during the first cycles of the measurement

3.3 Inspection of a whole string (dPL_S)

In order to test this methodology, and as a first attempt to validate it, we tested the case of two strings of just one panel (S=1) connected to a micro-inverter, with one of the panels being the defective panel shown in the previous figures. In this case, the electronic device was connected in series with the 1-panel string. Fig. 6 shows the dPL_S image for the case G = 800 W/m^2, nc=300, t_{exp}=8 ms, the On-Off signal differences and the measured current and voltage values for the inspected panel. As can be seen, an almost perfect square wave modulation is again obtained for the current intensity drawn from the inspected panel. The image quality is still good enough (SNR_{avg}=13.9) to distinguish the defective cells.

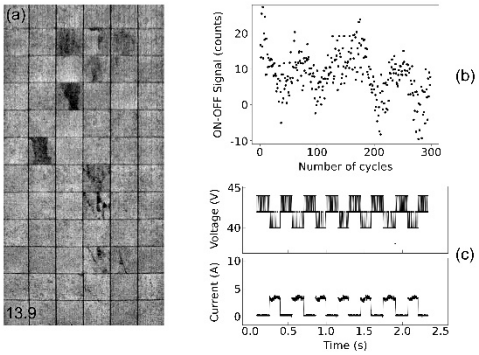

Figure 6: (a) dPL image of the same individual panel, with two panels connected to the micro-inverter, with the electronic device connected in series with the inspected panel (dPL_S) (G = 800 W/m^2, t_{exp}=8 ms, nc=300); (b) On–Off signal differences as a function of the number of cycles; (c) voltage and current values measured for the inspected panel during the first cycles of the measurement

It is also quite interesting to note that this dPL_S image provides different information about the defects in the cells. The dPL_S information is much more similar to the dEL image (Fig. 3(b)) with regard to the $dPL_{OC/SC}$ image (Fig. 3(a)). This result aligns with previous discussions about the information provided by dPL depending on the current drawn from the PV panels in the On and Off states, where the possibility of distinguishing a region's degree of isolation on a single dPL image was seen to depend on the level of current extraction and on the region's degree of isolation [12, 18]. This fact is now being studied in depth.

4 CONCLUSIONS

In conclusion, the electrical commutation described here does not change the state of the inverter. A very fast switching between the On and Off states can be performed by controlling the electronic device with wireless communication. The electronic device is a very cheap element that can be installed in the string and remain for the entire lifetime of the PV plant, if desired, allowing for the continuous monitorization of the state of the panels. The information provided by the dPL image is quite similar to the dEL. The filtration of the ambient light is properly performed, and the main defects of the solar cells of the panels can be detected. The method thus would allow for the inspection of solar plants, on-site, with the PV panels in operation, in a quiet contactless way, with a remarkably quality of the obtained images.

5 ACKNOWLEDGMENTS

This work has been financed by the Spanish Ministry

of Science and Innovation, under project PID2020-113533RB-C33, and by the Regional Government of Castilla y León (Junta de Castilla y León) and by the Ministry of Science and Innovation and the European Union NextGenerationEU / PRTR under the project "*Programa Complementario de Materiales Avanzados*". C. de Castro is grateful for the funding received through the "Investigo" Programme of the Ministry of Labour of the Government of Spain. K.P. Sulca is grateful for the funding received through the predoctoral contract programme of the University of Valladolid (2022), co-funded by the Santander Bank. C. Terrados is also grateful for the financial support received under project PDC2022-133419-I00, funded by MCIN/AEI/10.13039/501100011033 and NextGenerationEU/PRTR.

6 REFERENCES

[1] L. Koester, S. Lindig, A. Louwen, A. Astigarraga, G. Manzolini, D. Moser, Renew. Sustain. Energy Rev. 165 (2022) 112616.

[2] I. Høiaas, K. Grujic, A. Gerd, I. Burud, E. Olsen, N. Belbachir, Renew. Sustain. Energy Rev. 161 (2022) 112353.

[3] M. Köntges, S. Kurtz, C. Packard, U. Jahn, K.A. Berger, K. Kato, T. Friesen, H Liu, et al., IEA-PVPS Task 13: Performance and Reliability of Photovoltaic Systems. Subtask 3.2: Review of Failures of Photovoltaic Modules. Technical report, International Energy Agency (2014).

[4] M. Navarrete, L. Pérez, F. Domínguez, G. Castillo, R. Gómez, M. Martínez, J. Coello, V. Parra, in 31st Eur. Photovolt. Sol. Energy Conf. Exhib. (2015) p. 1989.

[5] O. Kunz, J. Schlipf, A. Fladung, Y.S. Khoo, K. Bedrich, T. Trupke, Z. Hameiri, Prog. Energy 4 (2022) 042014.

[6] L. Stoicescu, M. Reuter, J.H. Werner, in 29th Eur. Photovolt. Sol. Energy Conf. Exhib. (2014) p. 2553.

[7] J. Adams, B. Doll, C. Buerhop, T. Pickel, J. Teubner, C. Camus, C.J. Brabec, in 32nd Eur. Photovolt. Sol. Energy Conf. Exhib. (2015) p. 1837.

[8] S. Koch, T. Weber, C. Sobottka, A. Fladung, P. Clemens, J. Berghold, in 32nd Eur. Photovolt. Sol. Energy Conf. Exhib., (2016) p. 1736.

[9] G.A. dos Reis Benatto, N. Riedel, S. Thorsteinsson, P.B. Poulsen, A. Thorseth, C. Dam-Hansen, C. Mantel, S. Forchhammer, K.H.B. Frederiksen, J. Vedde, M. Petersen, H. Voss, M. Messerschmidt, H. Parikh, S. Spataru, D. Sera, in Proc. 44th IEEE Photovolt. Specialist Conf. (2017) p. 2682.

[10] M. Guada, A. Moretón, S. Rodríguez-Conde, L.A. Sánchez, M. Martínez, M.A. González, J. Jiménez, L. Pérez, V. Parra, O. Martínez, Energy Science & Engineering 8 (2020) 3839.

[11] L. Koester, A. Louwen, S. Lindig, G. Manzolini, D. Moser, Solar RRL 8 (2024) 2300676.

[12] M. Vuković, M.S. Wiig, G.A. dos Reis Benatto, E. Olsen, I. Burud, Prog. Energy 6 (2024) 032001.

[13] R. Bhoopathy, O. Kunz, M. Juhl, T. Trupke, Z. Hameiri. Prog. Photovoltaics Res. Appl. 26 (2018) 69.

[14] O. Kunz, G. Rey, M. K. Juhl and T. Trupke, IEEE 48th Photovoltaic Specialists Conference (PVSC), Fort Lauderdale, FL, USA, (2021) p. 0346.

[15] M. Vuković, M. Jakovljevic, A.S. Flø, E. Olsen, I. Burud, Appl. Phys. Lett. 120 (2022) 244102.

[16] M. Vuković, I.E. Høiaas, M. Jakovljevic, A.S. Flø, E. Olsen, I. Burud, Prog. Photovolt. Res. Appl. 30 (2022) 436.

[17] C. Mantel, G.A. dos Reis Benatto, N. Riedel, S. Thorsteinsson, P.B. Poulsen, H. Parikh, S. Spataru, D. Sera, Søren Forchhammer, in Proc. IEEE 7th World Conf. Photovolt. Energy Convers. (2018) p. 3285.

[18] G. Rey, O. Kunz, M. Green, T. Trupke, Prog. Photovolt., Res. Appl. 30 (2022) 1115.

[19] C. Terrados, D. González-Francés, V. Alonso, M.A. González, J. Jiménez, O. Martínez, J. Electron. Mater. 52 (2023) 5189.